Seasonality of African Precipitation from 1996 to 2009

BRANT LIEBMANN,* ILEANA BLADÉ,+ GEORGE N. KILADIS,# LEILA M. V. CARVALHO,@ GABRIEL B. SENAY,& DAVE ALLURED,* STEPHANIE LEROUX,** AND CHRIS FUNK++

* NOAA/Earth System Research Laboratory, and CIRES Climate Diagnostics Center, Boulder, Colorado
+ Departament d'Astronomia i Meteorologia, Universitat de Barcelona, Barcelona, Spain
# Physical Sciences Division, NOAA/Earth System Research Laboratory, Boulder, Colorado
@ Department of Geography and Earth Research Institute, University of California, Santa Barbara, Santa Barbara, California
& U.S. Geological Survey Earth Resources Observation and Science Center, Sioux Falls, South Dakota
** NOAA/Earth System Research Laboratory/National Research Council, Boulder, Colorado
++ Climate Hazards Group, Department of Geography, University of California, Santa Barbara, Santa Barbara, California

(Manuscript received 16 March 2011, in final form 30 September 2011)

ABSTRACT

A precipitation climatology of Africa is documented using 12 years of satellite-derived daily data from the Global Precipitation Climatology Project (GPCP). The focus is on examining spatial variations in the annual cycle and describing characteristics of the wet season(s) using a consistent, objective, and well-tested methodology. Onset is defined as occurring when daily precipitation consistently exceeds its local annual daily average and ends when precipitation systematically drops below that value. Wet season length, rate, and total are then determined. Much of Africa is characterized by a single summer wet season, with a well-defined onset and end, during which most precipitation falls. Exceptions to the single wet season regime occur mostly near the equator, where two wet periods are usually separated by a period of relatively modest precipitation. Another particularly interesting region is the semiarid to arid eastern Horn of Africa, where there are two short wet seasons separated by nearly dry periods. Chiefly, the summer monsoon spreads poleward from near the equator in both hemispheres, although in southern Africa the wet season progresses northwestward from the southeast coast. Composites relative to onset are constructed for selected points in West Africa and in the eastern Horn of Africa. In each case, onset is often preceded by the arrival of an eastward-propagating precipitation disturbance. Comparisons are made with the satellite-based Tropical Rainfall Measuring Mission (TRMM) and gauge-based Famine Early Warning System (FEWS NET) datasets. GPCP estimates are generally higher than TRMM in the wettest parts of Africa, but the timing of the annual cycle and average onset dates are largely consistent.

1. Introduction

By virtue of its geographical position, straddling the equator and extending into the subtropics of both hemispheres, Africa is a continent with large spatial contrasts in annual mean precipitation, epitomized by the presence of both some of the world's largest deserts and an extensive tropical forest. Africa also possesses a wide variety of precipitation regimes with sharp spatial transitions between them. These include tropical rain forest climates with no dry season, purely monsoonal regimes, regions characterized by two, roughly equal, wet seasons with almost no precipitation in between, regimes with a dominant and a minor wet season, desert systems, and even Mediterranean climates (Griffiths 1972). Because the distribution of precipitation throughout the year can be as important as total precipitation, it is important to document and understand these different regimes.

Although many studies have investigated multiple regional aspects of African precipitation, Africa as a whole has not been extensively studied. This paper seeks to provide a comprehensive description of some basic aspects of African precipitation climatology, focusing on annual distribution and temporal characteristics of the wet season(s). Our main objective is to compare the characteristics of precipitation throughout Africa as obtained from a uniform methodology and a consistent

Corresponding author address: Brant Liebmann, NOAA/ESRL PSD, Climate Diagnostics, R/PSD1, 325 Broadway, Boulder, CO 80305-3328.
E-mail: Brant.Liebmann@noaa.gov

DOI: 10.1175/JCLI-D-11-00157.1

dataset. Although precipitation estimates are obtained from only 12 years of high-resolution satellite data, the global dataset employed allows, for the first time, a spatially complete picture of the African continent. The paper also attempts to identify and describe the different rainfall regimes in more detail than has been previously attempted. Moreover, to assess which features are robust, the data are also compared with other estimates of precipitation.

One useful way to quantify the wet season is by its onset date, length, and rain rate (defined as the precipitation per day during the wet season). In addition to its scientific interest, a good understanding of the climatology and variability of these parameters could potentially be quite beneficial to agriculture (e.g., Ati et al. 2002; Hagos and Cook 2007; Cheung et al. 2008), as it could improve use of water resources over a continent that generally does not enjoy abundant and reliable rainfall. Furthermore, an accurate *prediction* of such quantities could help agriculture achieve maximum production through adjustment of crops and planting times (Ati et al. 2002).

Most studies of wet season onset over Africa, however, have been of regional scope and have not used a consistent methodology. Onset has been examined over West Africa (e.g., Sivakumar 1988; Le Barbé et al. 2002; Sultan and Janicot 2003; Marteau et al. 2009), Nigeria (Ati et al. 2002), Senegal (Camberlin and Diop 2003), and South Africa (Tadross et al. 2005) with almost as many different definitions for onset (e.g., Sivakumar 1992; Marteau et al. 2009). Moreover, these regional definitions were often tuned to capture onset in the specific area under study and are thus not applicable to the entire continent, preventing a comparison between regions. Global indices of local onset and retreat have also been developed for monsoonal regions (e.g., Zeng and Lu 2004; Zhang and Wang 2008), but these studies did not examine the African continent in detail. A primary purpose of this study is to apply an objective, sound, and robust methodology across the African continent to precisely determine the timing of onset. Those dates may then be composited to search for dynamical mechanisms related to onset.

Another important aspect of African precipitation is interannual variability, which regularly exceeds 20% of the long-term mean (e.g., Janowiak 1988; Nicholson 1993). As forecasts of interannual anomalies improve, it would be beneficial to understand whether, at a given location, such successful predictions involved a change in the timing and length of the wet season or its rate. While the short period of record used here (~12 yr) precludes more than a preliminary examination of interannual variability, we believe the methodology presented will be valuable in the future as longer records become available.

2. Precipitation data and climatology

The primary data for this study is the Global Precipitation Climatology Project (GPCP) One-Degree Daily (1DD) precipitation dataset (Huffman et al. 2001; Dinku et al. 2007). Several satellite products are combined to produce global precipitation estimates. There is a high mean absolute error for individual grid points (Huffman et al. 2001), although these errors are improved by spatial and temporal averaging. The available data extend from 1 October 1996 to 31 August 2009 (or 12 full years, 1997–2008). Gauge data are involved indirectly, as the 1DD data are scaled such that monthly totals match the GPCP monthly product, which includes gauge data (Dinku et al. 2007).

Figure 1a shows a map of mean precipitation, based on 1DD GPCC data. The Sahara Desert, occupying much of Africa's Northern Hemisphere landmass, receives less than 25 mm yr^{-1} over its driest region. Likewise, the Namib Desert of western Namibia is also extremely dry. In comparison, the wettest zones average more than 2 m yr^{-1}. The wet zone of Africa extends from about 10°N to 10°S across the western two-thirds of the continent. The maximum along the West African coast can be viewed as the easternmost extension of the Atlantic ITCZ, while the maximum centered near Mount Cameroon (~5°N, 10°E) corresponds to the western edge of the broad equatorial maximum, centered in the Congo basin, associated with the local Hadley cell. Even though most of the region receives less than 2 m yr^{-1} (Fig. 1a)—compared to more than 3 m yr^{-1} in the Amazon basin—discharge of the Congo River, whose namesake basin is entirely within the wet zone, is second to that of the Amazon River (Dai and Trenberth 2002). Farther to the east, annual precipitation decreases rapidly across the mountainous region east of Lake Victoria (elevations are shown in Fig. 1b). Away from the equator, in the Northern Hemisphere (NH), there is another isolated precipitation maximum over the Ethiopian Highlands (prominent in Fig. 1a). This mountainous region is often referred to as the water tower of Africa because of the many major rivers that emanate from it. In particular, more than 80% of the Nile flow originates in the northern Ethiopian Highlands (El-Fadel et al. 2003; Senay et al. 2009). In the Southern Hemisphere, there is also a zone of enhanced precipitation between about 10° and 20°S, extending southeastward and reaching a maximum in Madagascar, roughly consistent with the position of the South Indian convergence zone identified by Cook (2000).

These results are now compared with a corresponding map based on satellite measurements from the Tropical Rainfall Measuring Mission (TRMM) (e.g., Kummerow et al. 1998). The TRMM 3B42 daily data were

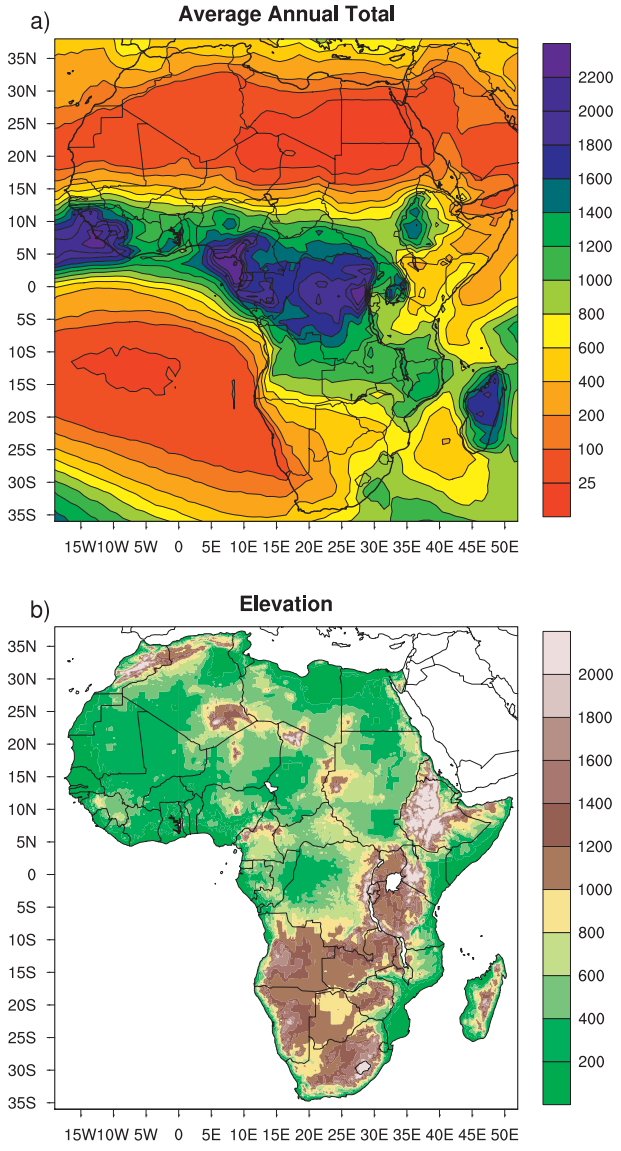

FIG. 1. (a) Annual average precipitation (mm) from 1997 to 2008 GPCP data. Note scale is not linear. (b) Elevation (m) of continent.

interpolated to match the GPCP grid and only years 1998–2008 were used. The major features of the TRMM long-term mean (Fig. 2a) agree with those obtained with the GPCP (Fig. 1a), even though the years included are slightly different. The differences between the two annual average estimates are shown in Fig. 2. In general, the GPCP indicates larger amounts than TRMM from 15°N to 15°S. In the eastern Congo and in western West Africa, for instance, GPCP mean precipitation is more than 700 mm higher than TRMM (as much as 170% of TRMM). The largest percent differences, however, are found around 20°N from the west coast to about 30°E, across the transition from the Sahel to the Sahara desert, with TRMM exceeding GPCC by more than twofold (and even threefold) at many locations.

A monthly precipitation dataset computed entirely from station records is also available: the U.S. Agency for International Development Famine Early Warning Systems Network (FEWS NET), also regridded to match GPCP from 12.5°S to 25.5°N. Station records include those from the Ethiopian National Meteorological Agency, the Centre Régional Agrhymet, the United Nations Food and Agriculture Organization, and the National Oceanic and Atmospheric Administration Global Historical Climatology Network. Still, coverage is sparse: if stations were evenly distributed, there would be one every 5000 km^2. Furthermore, the number of stations has decreased since the 1980s. When station observations are missing, the gridpoint values revert to the 1960–89 climatology. Thus, in many cases the gridpoint value represents more the climatology than the average of the 1998–2008 period. (The data and additional description can be found online at ftp://hollywood.geog.ucsb.edu/pub/FEWSNETInformingClimateChangeAdaptationSeries/FCLIM_TS/.)

Figures 3a,b show differences between the GPCP (TRMM) and FEWS NET annual totals. Both GPCC and TRMM tend to be high compared to FEWS NET across the West African Sahel, although the differences with GPCP are larger. On the other hand, along the southwest coast of West Africa, TRMM is substantially lower than either GPCP or FEWS NET. Over the eastern Congo, GPCP is high and TRMM is low relative to FEWS NET. Large GPCP excesses are also seen just northwest of the Ethiopian Highlands. In the complex topography of the highlands, GPCP and FEWS NET are in good agreement, while TRMM is low, but note that Dinku et al. (2007) found TRMM to be more reliable than GPCP there. Overall, in areas with large differences the gauge data often lie somewhere in between GPCP and TRMM, with GPCP biased high.

3. Defining the wet season(s)

The methodology used to determine the characteristics of the wet season is similar to that developed by Liebmann and Marengo (2001) for South America and Liebmann et al. (2008) for North America. To begin, one must determine the start of the climatological "water" or hydrologic year. At each grid point this is found by first calculating two quantities, the long-term annual-mean daily average and the long-term daily average for each day of the year (both in millimeters per day). Starting from 1 January (although any start date will produce the same result), the climatological daily average minus the climatological annual-mean daily average is summed (this is called the climatological

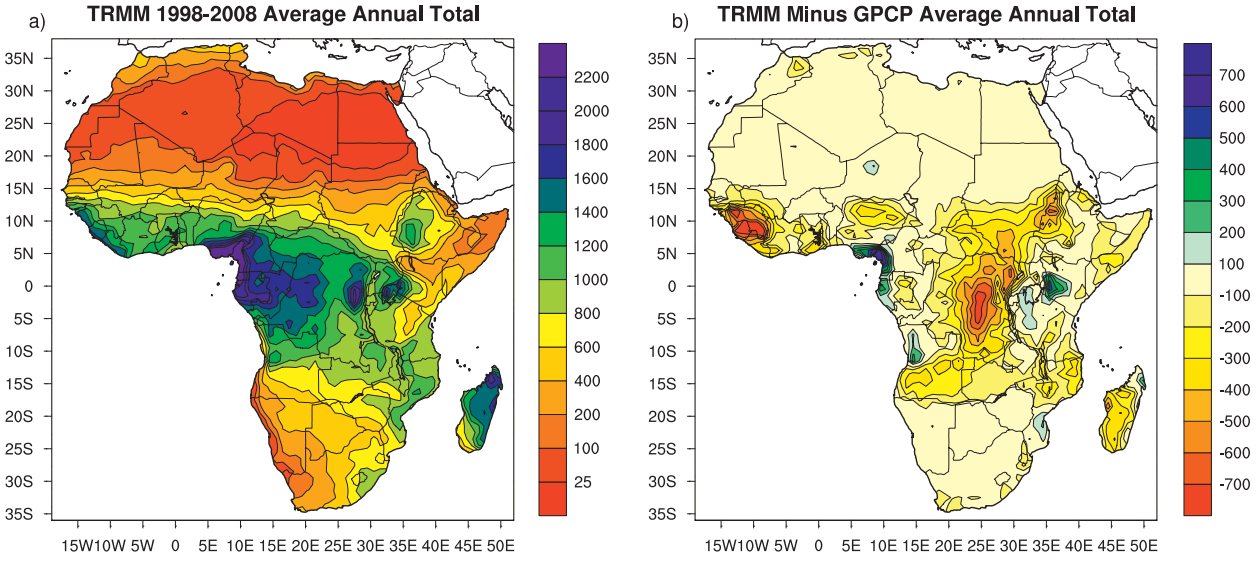

FIG. 2. (a) Annual average precipitation (mm) from TRMM for the period 1998–2008. (b) TRMM minus GPCP differences (mm) in annual averages for the same period.

anomalous accumulation). The first day past the minimum in this value is defined as the start of the water year because on this date climatological daily precipitation exceeds the annual average.

Once the climatological water year has been found, the onset for each year and each grid point can be determined. For each year of record, beginning 50 days prior to the start of the climatological water year and ending at the end of the climatological water year, daily precipitation minus the long-term annual-mean daily average is summed. This sum is called the "anomalous accumulation." The day after the value of the anomalous accumulation reaches its *absolute* minimum is taken to be the start of the wet season since, from that day onward for this particular year, accumulated precipitation (relative to onset) exceeds what would be expected from climatology. Conversely, the day on which anomalous accumulation is largest marks the end date of the wet season since following that day relative accumulation is less than expected from climatology. Wet season total, length, and rate are calculated from each year's start and end date.

The wet season definition described above and used throughout this paper was developed to provide a relatively objective method that can be applied uniformly because it depends on the local climatology. The only subjective aspect of our definition is the threshold requirement that precipitation exceed its local annual average for onset to occur. Moreover, the present definition accounts in an objective way for the problem of "false" onsets, as discussed below.

Most definitions of onset used in previous studies set an arbitrary fixed threshold requirement of continued rainfall to avoid a false onset. These criteria are designed for agricultural purposes so that onset dates may be used to determine optimal planting time by guaranteeing enough soil moisture during and after (Marteau et al. 2009). While they are likely appropriate for the region in question, they may not be adequate for other areas without additional tuning. For example, Marteau et al.

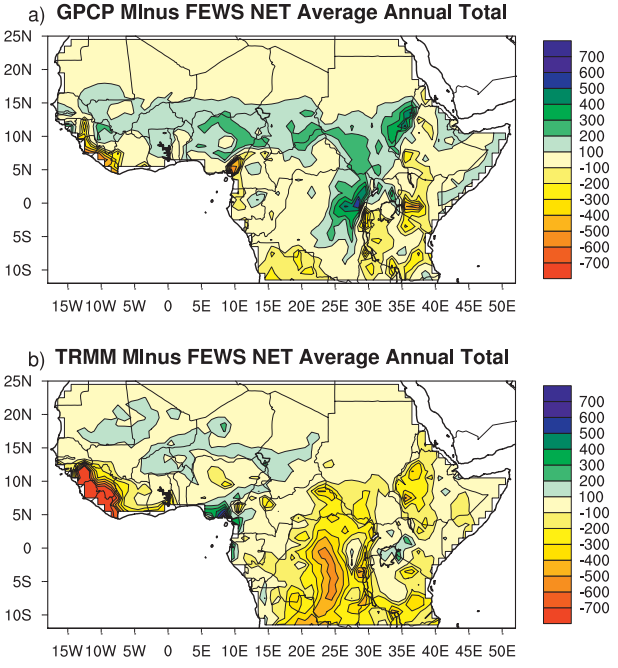

FIG. 3. (a) GPCP minus FEWS NET differences and (b) TRMM minus FEWS NET differences in annual total precipitation (mm) from quantities averaged during 1998–2008.

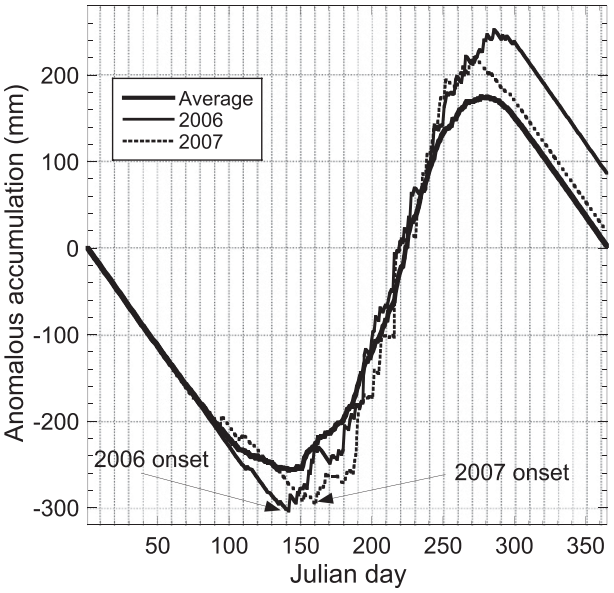

FIG. 4. Anomalous accumulation curves for the grid point at 12.5°N, 3.5°W (labeled C in Fig. 6) for climatology and years 2006 and 2007.

defines onset as the first wet day (1 mm or more) of one or two consecutive days totaling at least 20 mm without any 7-day dry spell (totaling less than 5 mm) during the 20 following days.

Instead, the no-dry-spell requirement is automatically accounted for in our algorithm because, if it is dry for an extended time, the anomalous accumulation value will dip below the value corresponding to the day that was the initial candidate for onset, thus disqualifying the original date. Moreover, the allowed duration of the dry period varies. If there is substantial rainfall at onset, the allowed dry period will be longer than if precipitation at onset barely exceeds the threshold (the climatological daily precipitation).

To illustrate the method, Fig. 4 shows the anomalous accumulation curve computed from the daily climatology, as well as curves for two individual years, at grid point 12.5°N, 3.5°W located within the Sahel semiarid region and whose monthly precipitation climatology is shown in Fig. 6 (point C). The annual cycle is typical of a monsoon regime with a single peak in summer and virtually no rainfall in winter. The climatological start and end dates of the wet season are 21 May and 29 September. These climatological onset and end dates (here and elsewhere in the paper) are determined by averaging onset and end dates for individual years. They generally differ only slightly from those determined directly from the climatological anomalous accumulation. The average wet season precipitation is 781 mm (again, computed as the average of each year's wet season). For this illustrative example anomalies accrue from 1 January. The 2007 wet season produced an average amount of precipitation (almost exactly), while 2006 received quite a bit more: almost 900 mm in total. Most of the difference can be explained by the fact that the 2006 season was 33 days longer (144 days) than the 2007 season (which was shorter than average) with both an earlier onset date and a later end date. The larger rain rate during the 2007 wet season compared to 2006 (7.0 vs 6.2 mm day^{-1}), however, partially compensated for the shorter season. Note that season 2007 exhibited a false start about 10 days prior to the real onset.

In the heart of the monsoon region, typified by the example in Fig. 4, the wet season is always defined and well behaved. In some (generally dry) areas, however, a problem occurs if the wet season for a particular year is extremely short and/or weak, or even absent. In those instances the anomalous accumulation curve will slope upward for only a brief period (short season) and/or exhibit such a modest maximum (weak season) that subsequently it will dip beyond the original minimum, or else it will be negatively sloped in the entire search interval (no wet season). Either way, the algorithm indicates the starting date of the wet season to be the last possible day of the search. To remove these spurious onset dates and locate the true onset date (if present), an alternative definition of onset is developed. For each day within the onset search interval, the number of days until the anomalous accumulation dips below the value on that reference day is counted. The day with the largest count is defined as onset. In general, onset dates from both methods agree. When and where these two definitions differ, the wet season is considered to be ''missing'' and that year is not included in the mean onset date calculation at that particular location. Also, start and end dates are set as missing if these are less than five days apart in order to avoid problems with brief bursts of rainfall that can occur at any time of the year in dry areas.

An indication of the extent to which the wet season, as defined here, captures precipitation in a given region is shown in Fig. 5, which depicts the percent of annual precipitation occurring in the wet season. Over much of the continent more than 80% of the annual total occurs within the wet season. The fraction is large between about 10° and 15° of latitude in both hemispheres and even larger (95%) at higher latitudes of the NH. In some regions, however, the wet season percentage is substantially lower. Along the equator, for example, extending eastward into the Horn of Africa, and also near the southern tip of Africa, this percentage falls below 50%. Generally, these are areas with two wet seasons or no distinct dry season, as will be documented below.

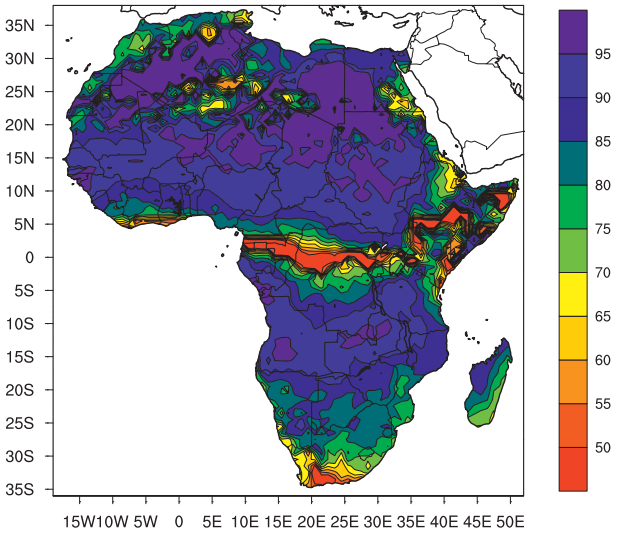

FIG. 5. Percent of annual total precipitation occurring in the wet season from GPCP: method for determining wet season is discussed in text.

4. Results

a. Annual precipitation distribution

Figure 6 shows the ratio of the second to first annual harmonic, computed from monthly climatologies, together with monthly climatologies at selected locations based on the GPCP, TRMM, and, where available, FEWS NET. The map gives an indication of where precipitation is evenly distributed throughout the year versus locations characterized by a single, sharp, wet season. There is some correspondence between a large first harmonic and a large percentage of rainfall contained within the defined wet season (Fig. 5) because single wet seasons are best captured by our methodology. In general, the second harmonic is relatively large near the equator, a reflection of the two wet seasons that occur following the two crossings of the solar zenith. For example, points marked D, E, and J in Fig. 6 all exhibit two annual peaks in precipitation.

It is interesting that at the Ivory Coast, near point D (5.5°N, 3.5°W), the double peak extends from 6.5°N to the equator (into the ocean, not shown), but in the SH there is only a single peak in March, decreasing with latitude (not shown). Although the timing of the maxima and minima agree, TRMM and FEWS NET both indicate nearly twice as much precipitation in June than in October, while the GPCP estimates comparable amounts in the two wet seasons. Also noteworthy is that, within the near-equatorial double maxima zone (point D), one of the annual minimums occurs in August—the same month where rainfall is *maximum* at this same longitude north of 10.5°N (points C and B)—which is consistent with the "jump" in the northward progression of the wet season discussed by Le Barbé et al. (2002) and Hagos and Cook (2007). This jump in the monsoon onset has been ascribed to inertial instability resulting from net moisture convergence into the region (Hagos and Cook 2007) and to teleconnections from the Indian monsoon associated with Rossby wave propagation (e.g., Janicot et al. 2009; Flaounas et al. 2010).

Within the Congo basin (e.g., point E in Fig. 6), the equatorial zone with its two annual peaks, is a region of transition from a regime with a single wet season in that hemisphere's summer to one with a single wet season in the opposite hemisphere's summer. A single summer wet season is thus observed poleward of 3.5°N and 3.5°S with the dry season becoming more pronounced with increasing distance from the equator. Near the equator, all precipitation datasets agree that the climatological wet season centered in November is always wetter than the one in April, but the difference is relatively small.

To the east the mountainous Lake Victoria region, source of the White Nile, has two roughly equal peaks in April and November, although the intervening months are not excessively dry (not shown). Indeed, western Kenya, located east of Lake Victoria, is wet enough year-round to produce rice as a primary crop (International Research Network 2005).

The most prominent second harmonic is found within the Horn of Africa (Fig. 6). Rainfall in this region, which is isolated from the rest of Africa by the Ethiopian Highlands and the Victoria Plateau (Fig. 1b), is substantially lower than in other near-equatorial regions (Fig. 1a). At point J (3.5°N, 41.5°E) in Fig. 6, representative of the region, the monthly climatology shows prominent peaks in April and October, evident in all datasets, separated by six months with almost no precipitation in between. The interannual standard deviation relative to the monthly climatology is quite large in that region (not shown). In particular, during October it exceeds the mean (ibid.).

Much of the rest of the tropics has a single summer wet season and a dry winter, characteristic of a monsoon regime (e.g., points B, C, H, I, and K in Fig. 6). Precipitation during the wet season generally tends to decrease with increasing latitude from the equator. For example, in the Sahel semiarid region [variously defined—see e.g., Nicholson et al. (1996); Hoerling et al. (2006)—but here considered to be ~12°–18°N, see points B and C in Fig. 6], the peak of the wet season occurs in August throughout (except in TRMM for which the peak at 17.5°N occurs in July), but the season is substantially wetter at 12.5°N than at 17.5°N.

Note, incidentally, that a large second harmonic does not always indicate the existence of two separate wet seasons. For instance, at point B in Fig. 6 (17.5°N, 3.5°W)

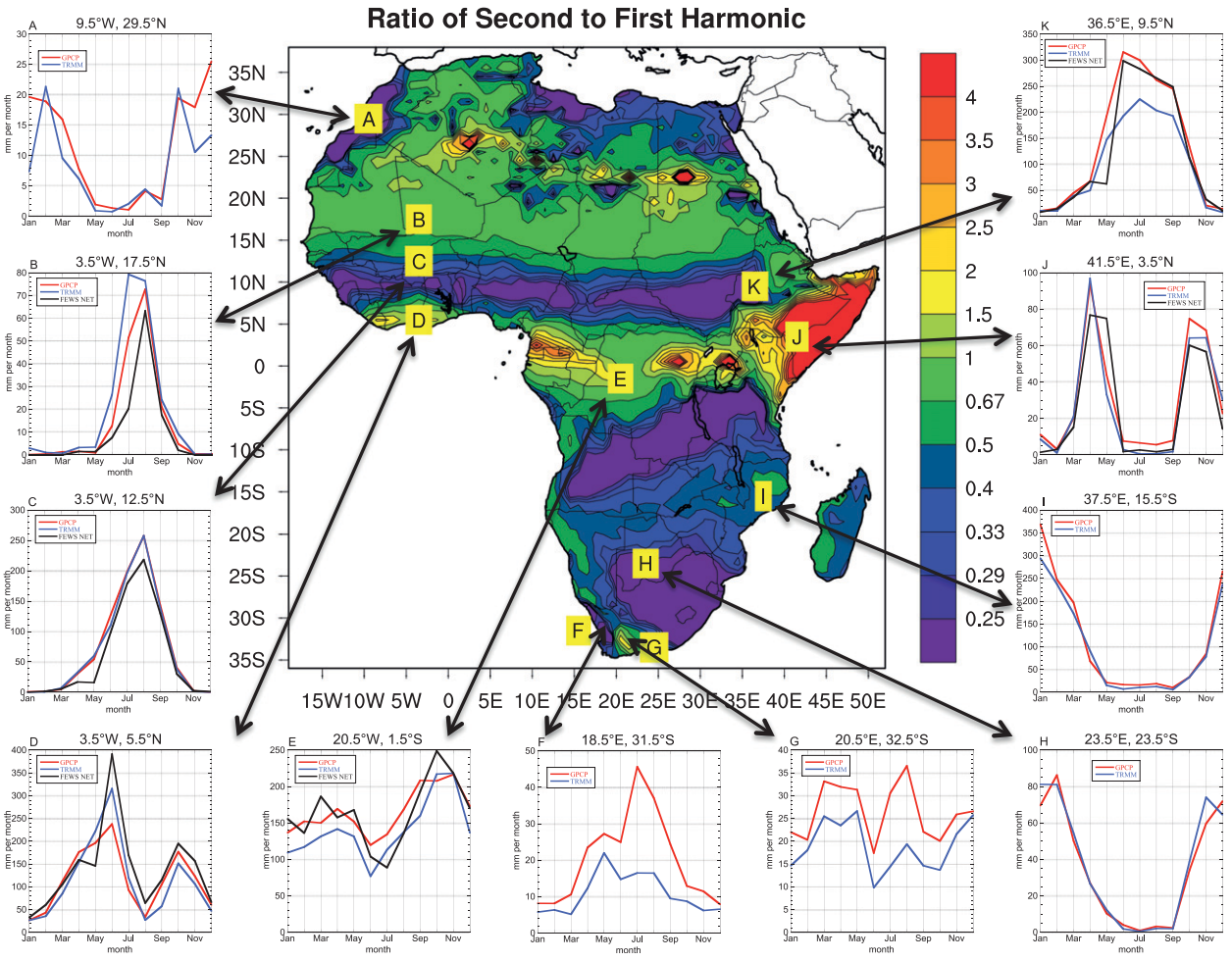

FIG. 6. Ratio of second to first annual harmonic computed from monthly climatologies. Graphs on perimeter show seasonal cycle of precipitation based on monthly averages (mm) at selected locations, for the period 1998–2008 for GPCP (red), TRMM (blue), and FEWS NET (black, where available).

there is a single wet season, yet the second harmonic has substantial amplitude. This is because the wet season is short enough that the annual cycle projects substantially onto the second harmonic.

An important transition occurs in the northern subtropics from a summer to a winter precipitation maximum. Africa's northern tier, from the Atlantic coast through the area north of the Atlas Mountains and along the Mediterranean coast of Libya and Egypt, exhibits a precipitation regime characterized by a winter maximum and a dry summer, typical of a Mediterranean climate (point A in Fig. 6). In the driest part of the Sahara (see Fig. 1), precipitation, when it does occur, is usually short lived and shows little seasonal preference.

In contrast with the northern subtropics, in the southern subtropics a prominent winter peak is observed only near the extreme southwestern coast (e.g., point F in Fig. 6). Throughout this narrow region, annual precipitation is low (Fig. 1a). The southeast–northwest oriented band, starting at the tip of southern Africa and extending to 25°S, characterized by a relatively large second harmonic (Fig. 6), marks the transition between a summer maximum to the north and east (e.g., point H) and a winter maximum to the west and south (point F). Point G (32.5°S, 20.5°E) is located in this transition zone; what little precipitation falls is evenly distributed throughout the year. At the southern tip of Africa, the defined wet season does not capture a large fraction of precipitation (Fig. 5).

The monthly averages shown in the bar graphs of Fig. 6 do not differ substantially between datasets, with a few exceptions. Differences generally involve amounts, rather than phasing, although TRMM appears to peak too early in the northern Sahel (point B). Along the southern coast of western Africa (point D), TRMM is 40% higher than

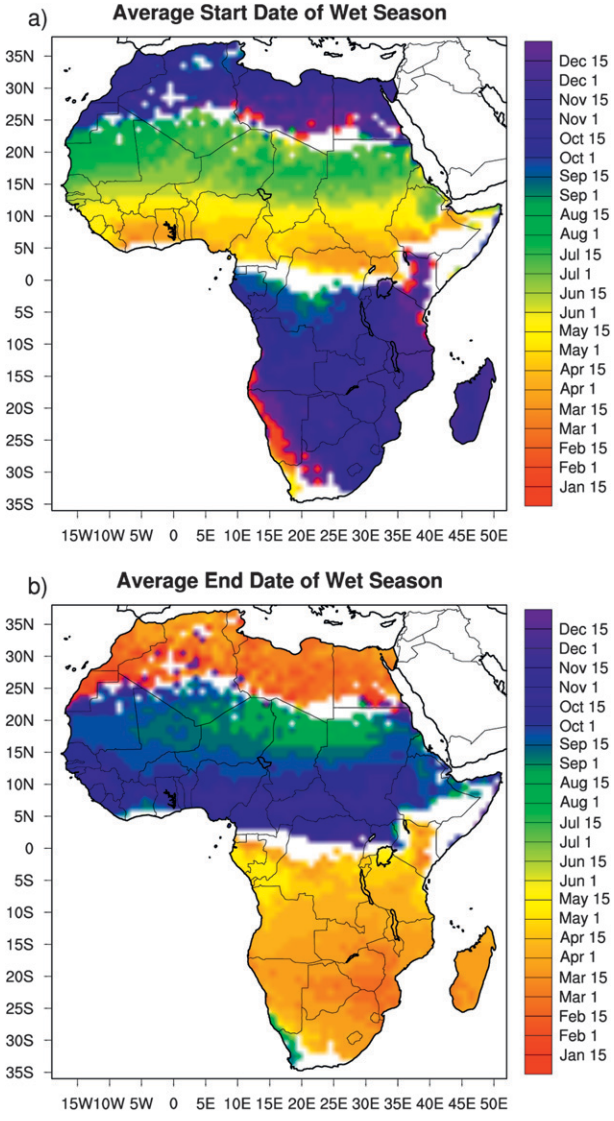

FIG. 7. Average (a) start date, computed from start dates of individual years, and (b) end date of wet season. Continental areas are masked if the ratio of second to first annual harmonic is greater than 4, the percent of annual total precipitation occurring in the wet season is less than 65%, or fewer than seven start dates are defined.

GPCP at the June maximum, and FEWS NET is higher still, but the timing of the wet seasons is consistent across datasets. Instead, in the higher latitudes of Africa with Mediterranean-like climates (points A and F), the GPCP indicates a maximum in midwinter that is absent in TRMM.

b. Characteristics of the wet season

Figures 7a and 7b show the average onset and end dates of the wet season. Some areas have been masked because there are multiple wet seasons (most pronounced in the eastern Horn of Africa), substantial precipitation falls outside the wet season, or onset is not robust (mostly in the Sahara Desert), and thus the technique is of limited value in those areas (see figure caption for details). The Horn of Africa, however, will be analyzed later using a modified definition of onset.

In general, the wet season begins in each hemisphere's early spring and spreads poleward, more rapidly in the Southern than in the Northern Hemisphere (Fig. 7a), with an equatorward withdrawal (Fig. 7b), again more rapid in the Southern Hemisphere. For instance, the wet season does not reach 20°N until boreal midsummer but is established throughout 20°S by late austral spring.

Onset and end in the region of enhanced annual precipitation over the Ethiopian Highlands (Fig. 1a) are in line with those at the same latitude to the east and west (Fig. 7). The climatological precipitation maximum in this area is thus a result of a locally increased wet season rate (not shown).

1) SOUTHERN AFRICA

Figures 8a and 8b are equivalent to Fig. 7 except they focus on Africa's Southern Hemisphere. The wet season expands from the southeast coast toward the west-northwest and from the Congo basin to the southeast throughout spring (Fig. 8a). Note that Fig. 8a has uneven contour intervals around 11 March that reflect a discontinuity in starting dates and the peculiar winter precipitation regime at the southwestern tip. The westward expansion of the wet season across southern Africa agrees with the progression of onset in this region, as determined by Tadross et al. (2005). As a result, the latest summer monsoon onset occurs along a northeast–southwest band passing through 17°S, 25°E.

The earliest ending of the southern wet season occurs in mid February at about 24°S, 30°E following which the dry season expands in all directions from there. (Again, while the contours make it appear as though there is a continuous withdrawal into the southwest corner, there is actually a discontinuity from April to June.) Withdrawal is not a mirror image of onset: the earliest withdrawal occurs north of the region of earliest onset (Fig. 8a), resulting in a long wet season along the east coast at around 30°S (Fig. 8c). Although the wet season rate is not exceptional (Fig. 8d), the long duration results in a local maximum in wet season (and annual) precipitation (Figs. 8e and 1a). The local maximum near the eastern coast at about 15°S, on the other hand, is the result of an enhanced rain rate (Fig. 8d) rather than a long season (Fig. 8c).

The TRMM minus GPCP average wet season total is shown in Fig. 8f. Wet season characteristics are computed

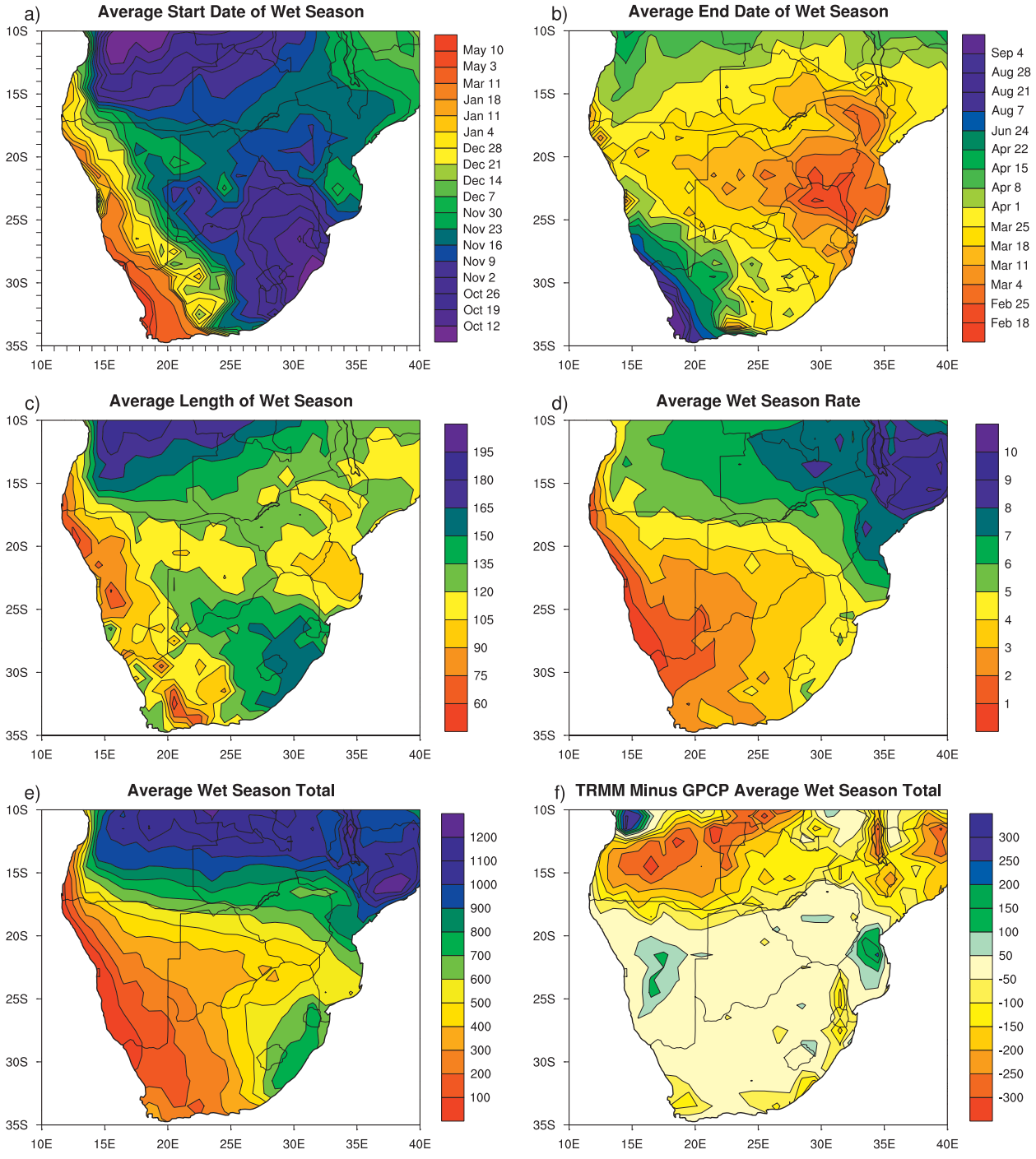

FIG. 8. As in Fig. 7a but for southern Africa. Note larger contour interval before and after 11 Mar. (b) As in Fig. 7b but for southern Africa. Note larger contour interval before and after 24 Jun. (c) Average length of wet season in days. (d) Average daily precipitation rate during wet season (mm day^{-1}). (e) Average wet season total (mm). (f) TRMM minus GPCP difference in average wet season total (mm).

for the exact same periods in each dataset, which includes wet seasons from 1998–99 to 2008–09. The differences are minor south of about 18°S, but to the north GPCP totals are substantially larger than TRMM. The wet season difference is the reason GPCP annual totals are larger than TRMM (Fig. 2b). This wet season difference is the result of both a higher wet season rate and longer wet season in GPCP than TRMM (not shown).

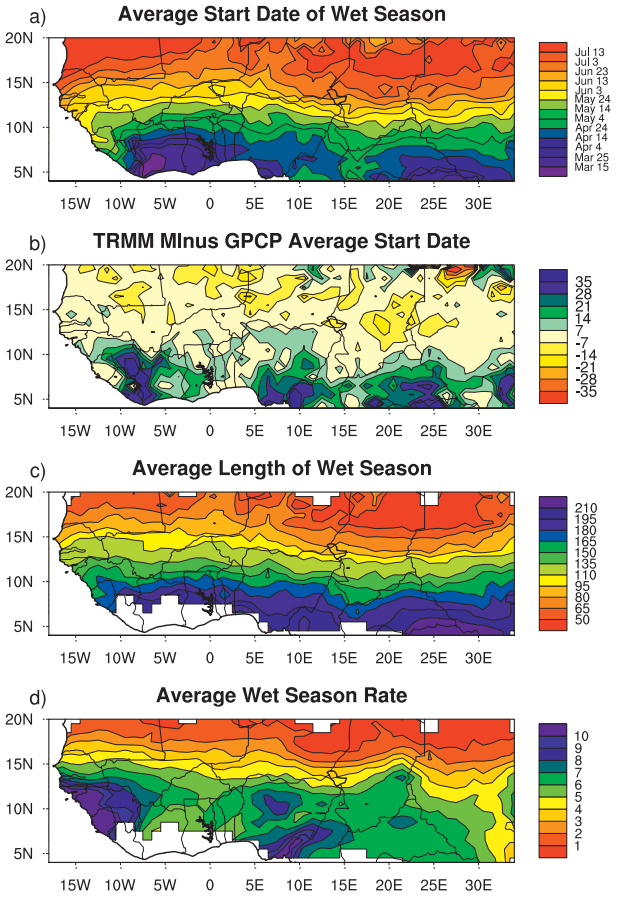

FIG. 9. (a) Average start date of wet season for western/central Africa. (b) TRMM minus GPCP difference in average start day (days). (c) Average length of wet season in days. (d) Average daily precipitation rate during wet season (mm day^{-1}). In (c) and (d) continental areas with less than 80% of annual precipitation occurring during the defined wet season are masked.

2) WEST AND CENTRAL AFRICA

West Africa and the western Sahel have been studied more extensively than other parts of the continent (e.g., Nicholson 1980; Nicholson et al. 1996; Redelsperger et al. 2006; Hagos and Cook 2007; Janicot et al. 2008; Marteau et al. 2009), but few studies have focused on central Africa. Recently, West Africa has been the subject of several field campaigns, as part of the African Monsoon Multidisciplinary Analysis (AMMA) program, with particularly intense field activity in 2006 (e.g., Redelsperger et al. 2006; Lebel et al. 2010).

Figure 9 is focused on western and central Africa. The wet season begins near the southernmost coast of West Africa in early March (Fig. 9a). Although this region was masked in Fig. 7 because the defined wet season does not capture a large fraction of the annual total, onset here is robust and reflects the start of the primary wet season. This area of early onset coincides with a local minimum in annual precipitation (Fig. 1a). Onset occurs somewhat later to the east, and still later to the northwest, in the vicinity of the observed local maximum in annual precipitation.

North of about 10°N the wet season progresses relatively evenly northward, at least on average, although Marteau et al. (2009) found little spatial coherence on interannual time scales in the western Sahel. Moreover, close inspection reveals that from 10° to 15°N onset dates west of about 5°E occur about a month earlier than east of about 10°. In the west, dates are in reasonable agreement with those determined by Le Barbé et al. (2002) using a different definition for onset. Over the western Sahel the relative sense of onset is also consistent with the dates determined by Marteau et al., although their average onset dates appear to be about two weeks later than those determined here, primarily due to a higher threshold compared to ours (their definition of onset is given in section 3).

Figure 9b shows the TRMM minus GPCP average onset date. South of 10°N onset occurs earlier in the GPCP than in TRMM, by more than one month in some areas. In the region of largest discrepancy, near (9°N, 9°W), GPCP amounts are close to FEWS NET's in each month, while TRMM is substantially lower (not shown). Most importantly for onset, the ramp up in GPCP occurs earlier than TRMM.

The average wet season end is not shown because withdrawal is relatively uniform with longitude, except west of about 5°W, where it occurs later than to the east. The wet season withdraws more rapidly than it begins. Furthermore, the GPCP and TRMM are in good agreement for the most part, except TRMM ends earlier in the area along the west coast where annual totals are quite different (Fig. 2b).

The length of the wet season is shown in Fig. 9c. The map is masked where less than 80% of annual precipitation is contained within the wet season. This mainly masks the southern coast of West Africa where there is a secondary wet season after a minimum in August (see point D of Fig. 6). Length varies sharply in latitude, with the wet season generally lasting over half a year south of about 9°N but only 50 days at 20°N. The length of the wet season at a given latitude is about a month longer west of 5°E than east of 10°E, a reflection of the earlier onset date in the west. Differences between GPCP and TRMM (not shown) are mostly due to differing onset dates.

The wet season rain rate (Fig. 9d) exhibits large variations in longitude near 10°N with the largest rates found along the west coast. These rates are twice as large as to the east and more than compensate for the short season (Fig. 9c), resulting in high annual totals (Fig. 1a).

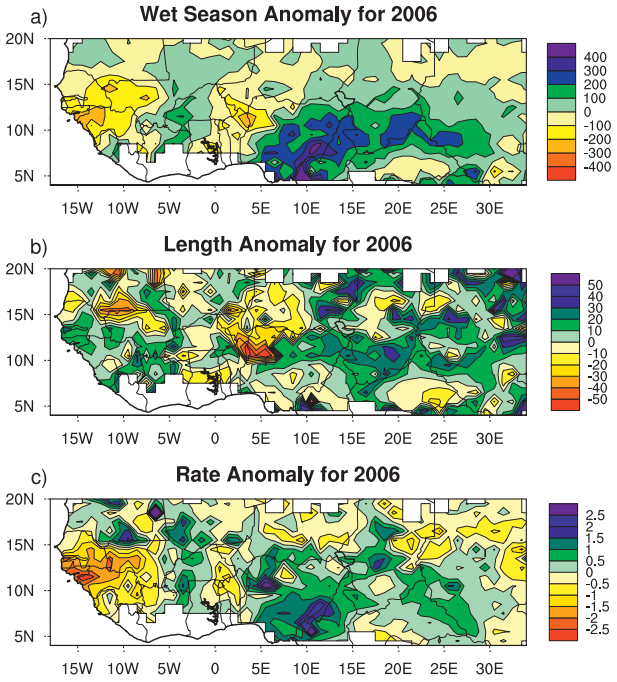

FIG. 10. Anomalies for 2006 in (a) wet season total (mm), (b) length (days), and (c) rate (mm day^{-1}). Continental areas with less than 80% of annual precipitation occurring during the defined wet season are masked.

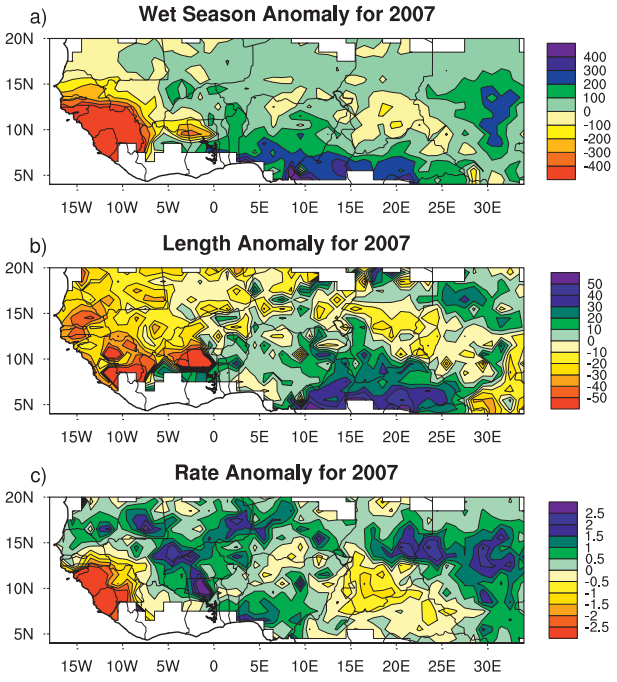

FIG. 11. As in Fig. 10 but for year 2007.

High rates in TRMM are narrowly confined to the coast (not shown).

As an example of how anomalous West African precipitation characteristics vary on an interannual basis, Fig. 10a shows the wet season precipitation anomaly for year 2006, the focus year of the field component of the AMMA project. Most of West Africa exhibits near-average precipitation (see also Janicot et al. 2008), while central Africa, south of about 13°N, received substantially more than average (between 100 and 300 mm more). The anomaly in wet season length is shown in Fig. 10b. The largest deviations in length (~50 days) result from early start dates, as end dates are close to climatology (not shown). Rate anomalies, shown in Fig. 10c, indicate that the wet season surplus in central Africa, east of 5°E, resulted from both an anomalously long and rainy season. On the other hand, along the west coast the deficit was entirely due to a low rate as length anomalies are positive in that region.

The 2007 wet season was the driest of the 1997–2008 GPCP record in the west (Fig. 11a), while east of the Greenwich meridian precipitation was near average except in the far south and east of the domain. During this season both length (Fig. 11b) and rate (Fig. 11c) anomalies contributed to dryness in the west. Instead, in the south only length anomalies led to the above-average precipitation, while in the east a large rain rate was responsible for the surplus near 30°E.

TRMM and GPCP annual anomalies for 2006 and 2007, relative to their respective 1998–2008 average, are shown in Fig. 12. While there are broad similarities between the patterns of anomalies for each year, there are large differences in detail. In 2006, for example, TRMM (Fig. 12a) indicates extremely large negative anomalies along the southwest coast compared to GPCP (Fig. 12b), and that is on top of an already drier average in TRMM (Fig. 2b). The following year, however, both TRMM and GPCC exhibit large dry anomalies in that same region, more pronounced in GPCC (Figs. 12c,d). Thus, differences between datasets cannot be accounted for by bias alone. Indeed, in 2006 at about 25°E, anomalies are generally of opposite sign in the two datasets.

Based on interannual point-by-point correlations (not shown), the length of the wet season and its rate appear to be largely independent. Correlations of wet season total versus length and rate reveal a tendency for length to be the controlling factor in the south of the domain (also not shown). Instead, variations in rate explain the most variance in wet season total throughout most of the Sahel and in the region of recurrent large anomalies along the west coast (Fig. 12), as illustrated for year 2007 in Fig. 11a. The limited number of years available, however, results in most of the correlations being not statistically significant.

We will now try to identify common dynamical patterns leading to onset for the results could help prediction of

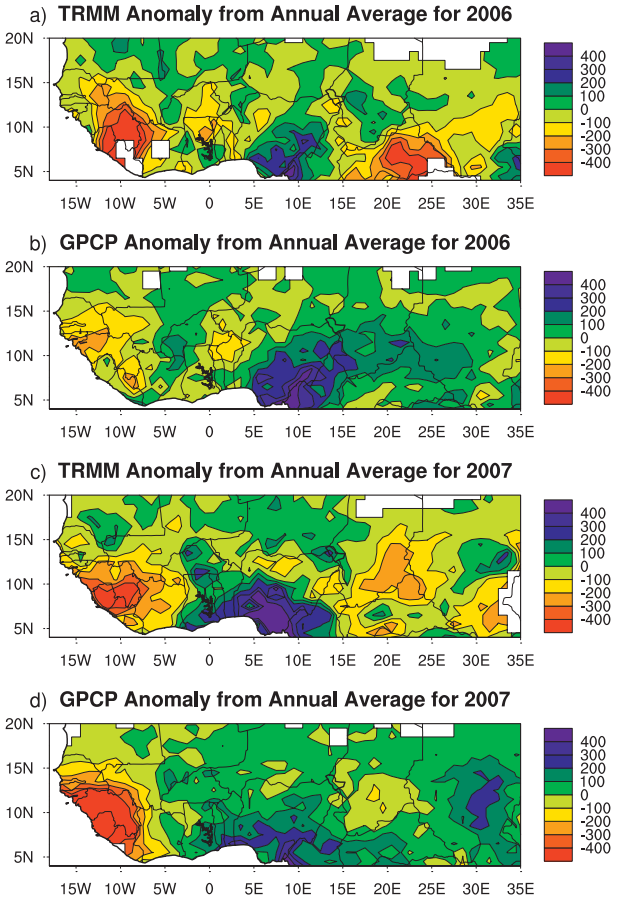

FIG. 12. Anomalies of annual totals relative to the 1998–2008 average (mm) for (a) TRMM and (b) GPCP in 2006 and for (c) TRMM and (d) GPCP in 2007.

onset date. Figure 13 shows composited fields relative to the day of onset at 12.5°N, 3.5°W. GPCP precipitation is shaded, TRMM precipitation is contoured, and the vectors represent 30-day high-pass filtered National Centers for Environmental Prediction reanalysis 200-hPa winds. From day −4 to day −3, precipitation decreases over South America and increases over the western and central Atlantic (Figs. 13a,b). This zonally elongated band of precipitation suggests that an active ITCZ is still strongest in the western Atlantic on day −2 (Fig. 13c). On day −1 (Fig. 13d) the heaviest precipitation has moved to the central Atlantic. At onset (Fig. 13e), there is light precipitation over the African continent and more over the eastern Atlantic. The heaviest precipitation occurs at the coast on day +1 (Fig. 13f). The entire sequence gives the impression of a disturbance propagating eastward along the axis of the ITCZ from South America to the Guinea coast, suggesting the possibility that a convectively coupled Kelvin wave is involved (e.g., Wang and Fu 2007; Mekonnen et al. 2008). Certainly, Kelvin waves have been implicated in at least one instance of monsoon onset over West Africa (Mounier et al. 2008).

The contours of TRMM align quite closely with those of GPCP in Fig. 13, even though the TRMM composite does not include year 1997. That is in part because the onset sequence for each year (not shown), although noisy, resembles the composite. While this may be the best composite example of eastward propagation along the ITCZ associated with onset, composites at other latitudes in western Africa also show eastward movement within the ITCZ. This example thus highlights the potential for prediction of monsoon onset over Africa using the datasets and techniques outlined in this study.

3) EASTERN HORN OF AFRICA

The eastern Horn of Africa, taken here to include eastern Ethiopia and the coastal plain of Somalia and eastern Kenya, is interesting for its strong semiannual cycle associated with two wet seasons, which occur between March and June (e.g., Camberlin and Philippon 2002; Williams and Funk 2011) and between September and December (e.g., Hutchinson 1992). These wet seasons, referred to as March–June and September–December hereafter (although the timing and names vary regionally), result from the northward and southward movement of the Indian Ocean ITCZ (Hutchinson 1992; Bowden and Semazzi 2007). In Somalia most crops are planted in spring (Hutchinson 1992), as the March–June wet season is generally wetter and traditionally considered more reliable than the September–December season. Indeed, in the September–December wet season some parts of Somalia experience crop failure in one of three years (Hutchinson 1992). Some of the September–December interannual variability is explained by a moderate relationship with the Southern Oscillation (Ogallo et al. 1988), whereby weak rainfall tends to occur in years with a high SOI index or La Niña conditions (Kiladis and Diaz 1989; Hutchinson 1992).

As previously mentioned, precipitation in the eastern Horn is relatively low compared to the rest of the near-equatorial belt, ranging from less than 200 mm yr^{-1} in the north to somewhat more than 700 mm yr^{-1} along the Kenya coast (Fig. 14a). As over much of the equatorial belt, GPCP estimates tend to exceed both TRMM (Fig. 14b) and FEWS NET (Fig. 14c). To examine the characteristics of each wet season, the March–June season is assumed to begin as early as 1 January and end as late as 29 July in the onset search algorithm, while the September–December wet season is allowed to occur between 15 June and 12 January. The areas in which the ratio of the amplitude of the second to the first harmonic is less than 0.75 are set to missing.

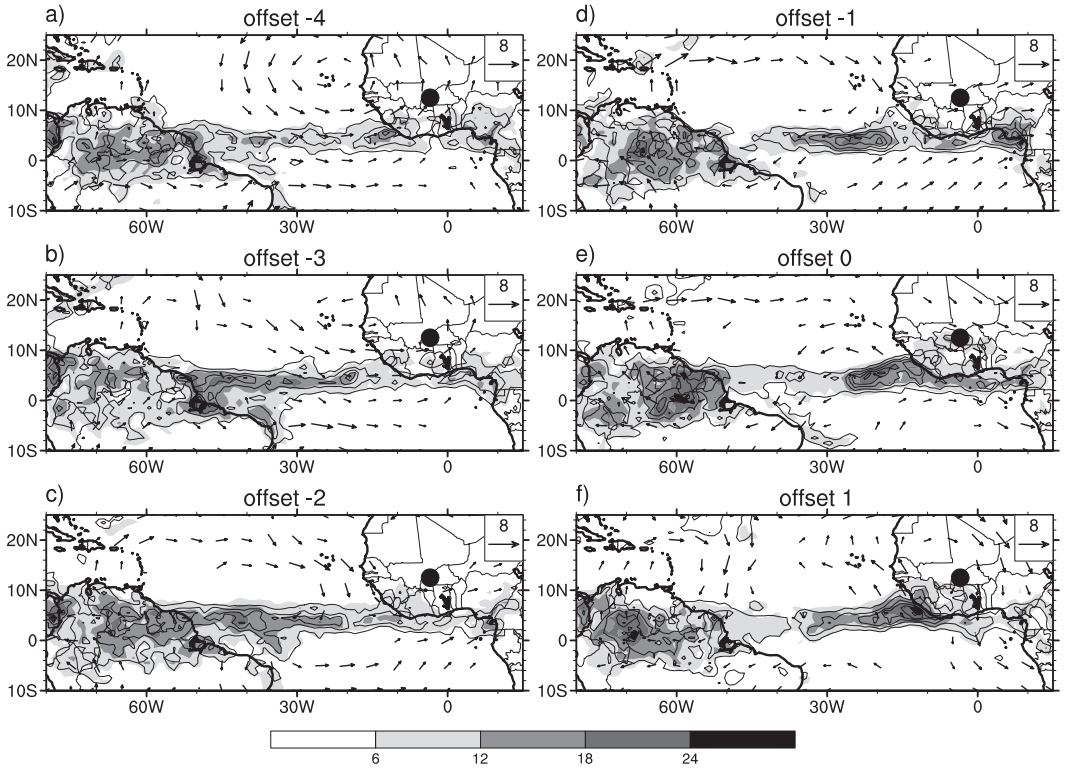

FIG. 13. Composite of GPCP precipitation (shaded), TRMM precipitation (contoured, interval 6 mm day^{-1} with zero contour omitted and negative contours dashed), and 30-day high-pass 200-hPa wind vectors relative to onset at 12.5°N, 3.5°W (dot).

The March–June wet season spreads rapidly almost due eastward toward the tip of the Horn from about 37.5°E in early April to the entire peninsula by mid-to-late April (Fig. 15a). Average onset as depicted by TRMM (Fig. 15b) is within 10 days of GPCP over most of the domain. The precipitation rate (Fig. 15c) during the March–June wet season varies from less than 3 mm day^{-1} in the north to more than 10 mm day^{-1} in south-central Somalia. The GPCP rate generally exceeds TRMM except in the south (not shown). The ''bull's-eye'' at 45°E is also not evident in TRMM (not shown), although the swath of high rates extending to the southwest is.

The March–June wet season length (Fig. 15d) ranges from less than a month in the north, near the coast, to more than double that at the south coast and in the western interior. Although there are isolated points throughout the domain with length differences of 20 days or so between GPCP and TRMM, TRMM lengths are systematically longer only in the north (not shown). The March–June season total (Fig. 15e) is less than 100 mm in the north but more than 400 mm along the coast of Kenya. Except in the vicinity of the bull's-eye in GPCP rate, GPCP and TRMM seasonal totals are within 50 mm of each other throughout most of the domain (Fig. 15f).

The September–December wet season (Fig. 16a) spreads southward from the north coast in early September and arrives at the equator in mid October. Withdrawal (Fig. 16b) is roughly opposite so that, even though the rate (Fig. 16c) decreases with increasing latitude, the length (Fig. 16d) is roughly uniform in space; therefore, the wet season total distribution (Fig. 16e) mimics that of the rate. Differences in the length and rate between GPCP and TRMM are usually small, except for several isolated grid points (not shown). Consistently, the pattern of differences in the wet season total (Fig. 16f) is rather bland and similar to that in March–June (Fig. 15f).

Figures 17 and 18 show composites of GPCP (shaded), TRMM (contoured), and 30-day high-pass 850-hPa wind relative to onset for the March–June and September–December wet seasons at 3.5°N, 41.5°E. In both composites the GPCP and TRMM alike show the entire eastern Horn to be almost completely dry up to the day of onset. The wet conditions observed at onset (Figs. 17e and 18e) remain on day +1 (Figs. 17f and 18f) and beyond (not shown). At onset most of the precipitation in the eastern Horn is located south of the base point in the March–June composite (Fig. 17e) and north of the base point in the September–December composite (Fig. 18e), consistent with the progression of onset in each of

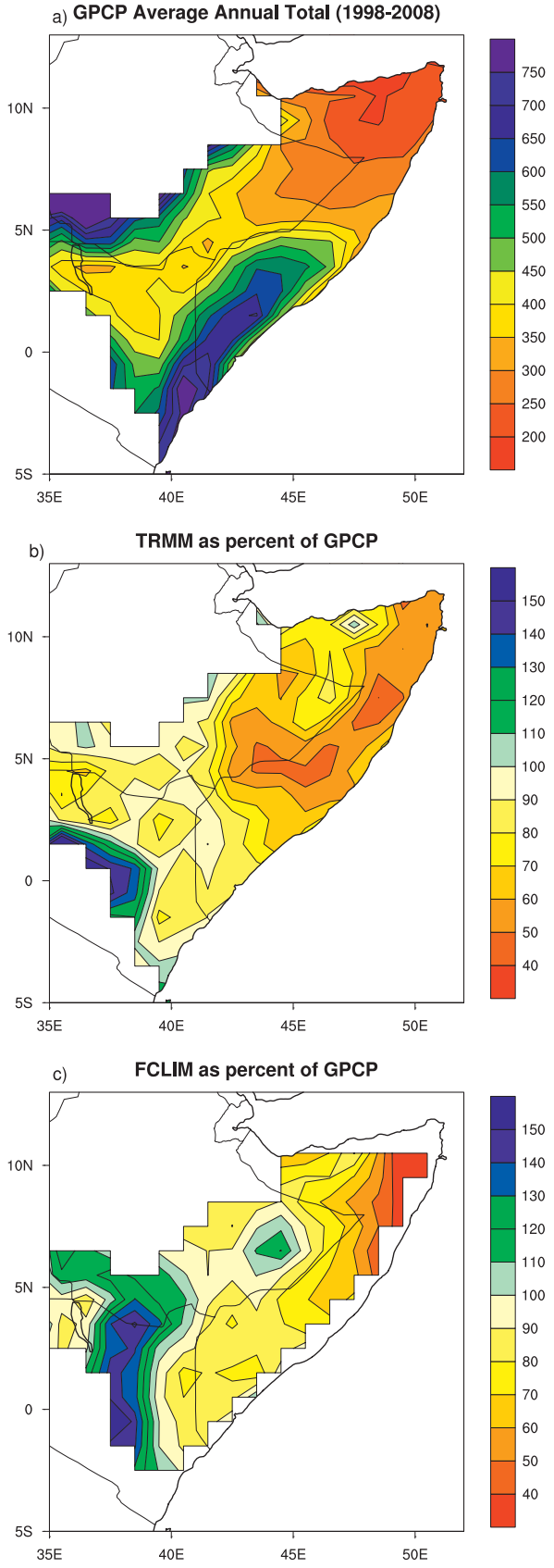

those seasons (Figs. 15a and 16a). In both composites there is a suggestion of precipitation expanding from the west at onset, perhaps propagating eastward along the equator, but the composites are noisy. While GPCP and TRMM are qualitatively consistent with each other in that average onset is evident on the same day in both, the amounts and pattern details vary substantially.

5. Summary and discussion

The motivation of this study was to document annual mean precipitation, seasonal variations, and wet season characteristics, focusing on onset over the entire African continent, using a consistent methodology and complete global dataset. Such a global analysis of the African wet season has not been attempted before. GPCP high-resolution daily precipitation, which extends from late-1996 to mid-2009, is the primary data source for this study, but the results are also checked against those obtained using TRMM and FEWS NET.

Large areas of Africa receive inadequate or unreliable rainfall. Based on GPCP only the coast of West Africa, the mountainous region near the Cameroon–Nigeria border, and isolated spots in the Congo basin receive more than 2 m yr^{-1}, and less than 1 m yr^{-1} occurs over vast areas. Moreover, in the wet regions near the equator these estimates may be biased high, as the GPCC tends to indicate more precipitation than either TRMM or FEWS NET. In particular, in the eastern Congo and Guinea coast, GPCP exceeds TRMM by more than 700 mm.

The timing of the wet season is documented using a consistent, objective, and well-tested definition of onset. Basically, onset is said to occur when daily precipitation consistently exceeds its local annual daily average and ends when precipitation systematically drops below that value. Throughout most of Africa a large fraction of rain falls in a single summer wet season with a well-defined onset and end. In the NH the wet season progresses northward throughout spring. Progression in the SH is not symmetric: the wet season advances southward until about 18°S, but farther south it proceeds northwestward from the southeast coast so that the latest onset is found at about 18°S, 15°E in late spring/early summer. Another interhemispheric asymmetry is found in subtropical regions: unlike the tropics, the northern tier of the continent exhibits a single precipitation maximum in winter,

←

FIG. 14. Average (a) GPCP annual total precipitation (mm) for the period 1998–2008 and for (b) TRMM and (c) FEWS NET as percent of GPCP for same period.

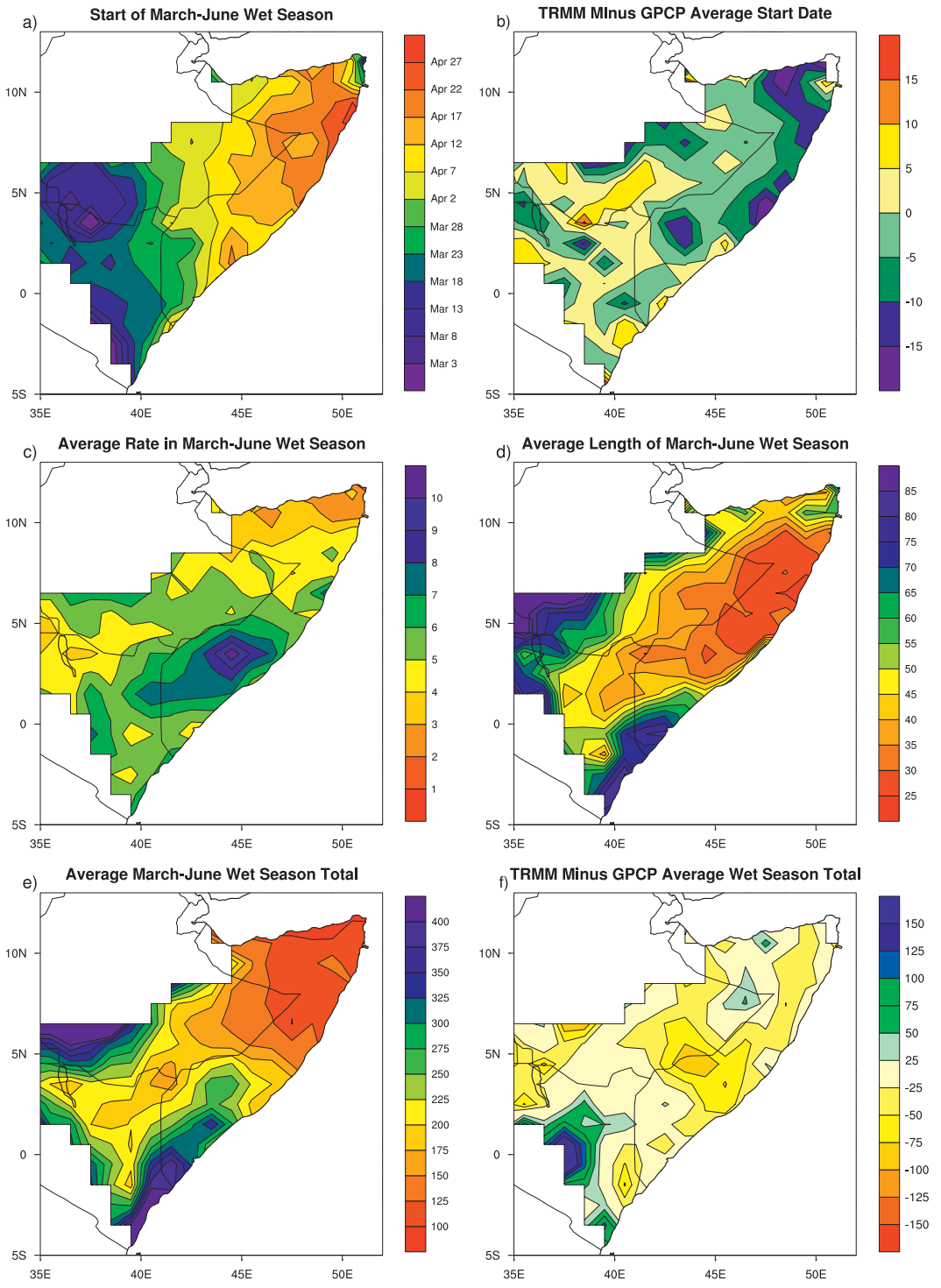

FIG. 15. (a) Average start date of March–June wet season. (b) Average TRMM minus GPCP difference in start date for March–June wet season (days). (c) Average rate of March–June wet season (mm day^{-1}). (d) Average length of March–June wet season (days). (e) Average March–June wet season total (mm). (f) Average TRMM minus GPCP difference in March–June wet season total (mm). Areas with ratio of second to first annual harmonic less than 0.75 are blank.

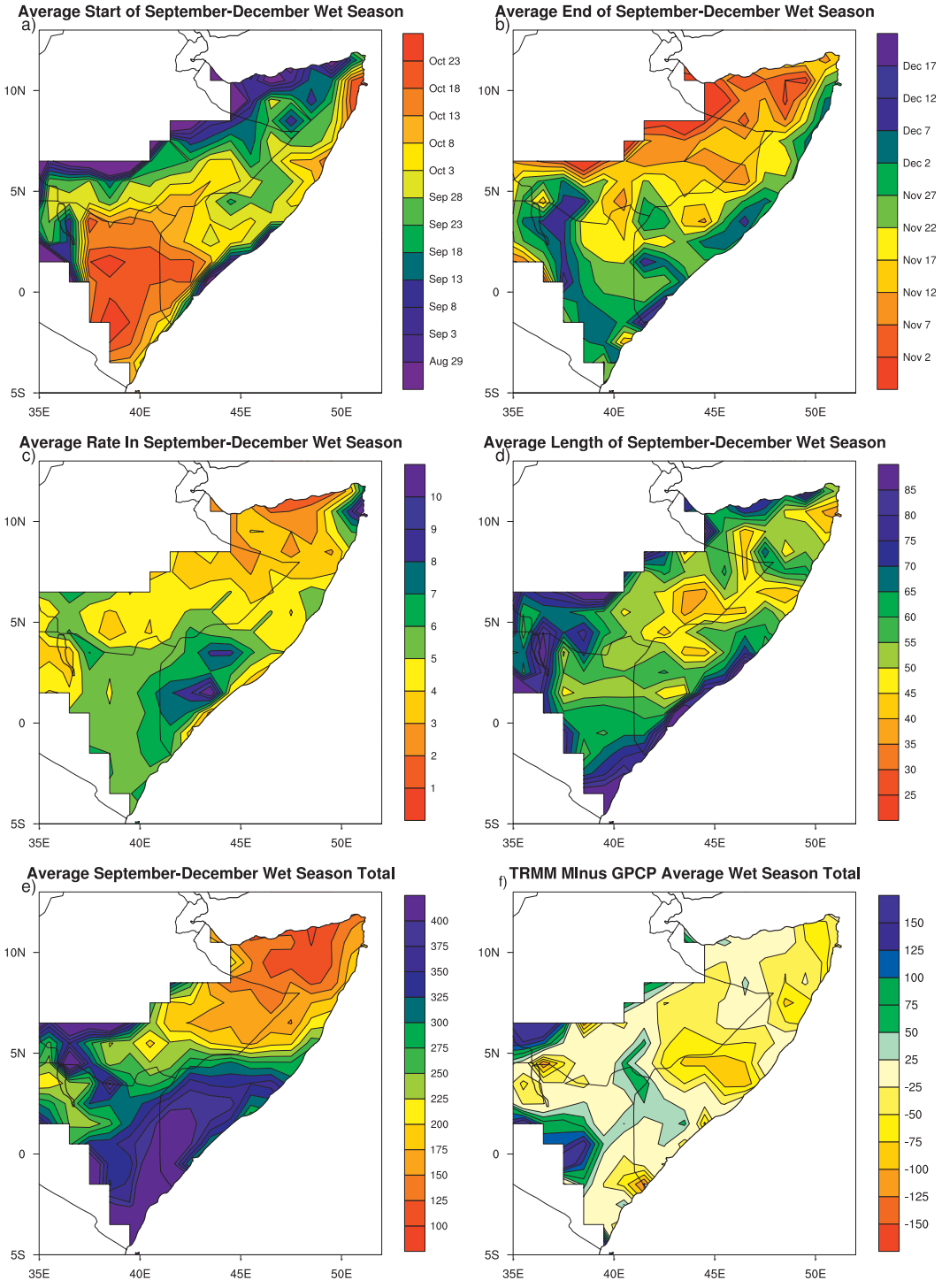

FIG. 16. (a) Average start date of September–December wet season. (b) Average end date for same season. (c) Average rate (mm day^{-1}) for same season. (d) Average length (days) for same season. (e) Average wet season total (mm). (f) TRMM minus GPCP difference in wet season total for September–December season.

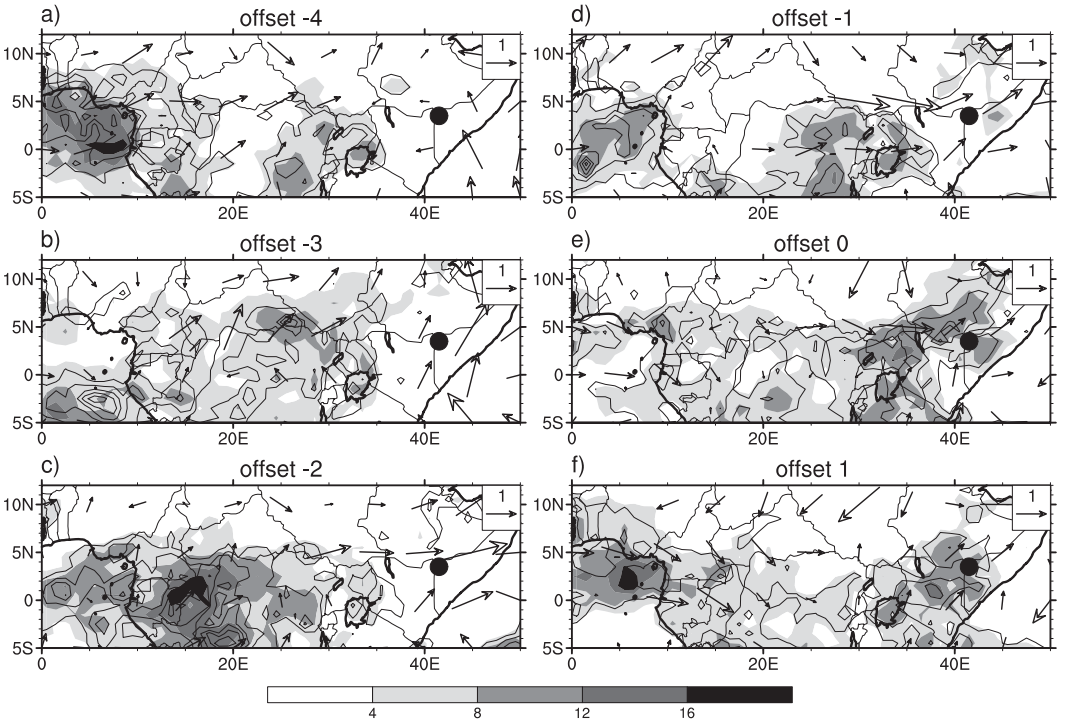

FIG. 17. Composite of GPCP precipitation (shaded), TRMM precipitation (contour interval 4 mm day^{-1}), and 30-day high-pass 850-hPa wind vectors relative to onset of the March–June wet season at 3.5°N, 41.5°E (dot).

but in the SH this Mediterranean-like regime is only found in a narrow region along the extreme southeastern coast.

Equatorial Africa often exhibits two wet seasons and a relative abundance of precipitation. There, the interval between the wet seasons is characterized by reduced, but not insignificant, rainfall. An exception to equatorial rainfall abundance lies in the region ringed to the west by the Ethiopian Highlands and by the mountainous region that includes Mount Kilimanjaro and Mount Kenya (Fig. 1b). This region spans the equator, yet is semiarid to arid. The focus here has been on the part of this domain—approximately the easternmost Horn of Africa—that exhibits a strong semiannual cycle of precipitation (Fig. 6) with completely dry conditions between the two wet seasons. The detailed figures of onset (Figs. 15a and 16a) and end (Fig. 16b) show a pattern clearly consistent with a northward ITCZ displacement in spring and southward in fall. Nevertheless, the connection between the ITCZ, as a continuously migrating zone of precipitation, and the wet season in this region is tenuous in climatological maps of monthly precipitation (not shown).

At selected locations in the Sahel and eastern Horn (Figs. 13, 17, and 18), onset is associated with enhanced precipitation approaching from the west. In particular, the composite relative to a Sahel grid point (Fig. 13) suggests that onset is preceded by an eastward propagating disturbance that intensifies the ITCZ as it crosses the Atlantic and moves into Africa.

No immediate conclusion can be drawn as to which dataset best represents African precipitation. On annual scales, if one assumes the FEWS NET gauge network to be the most reliable, the GPCP and TRMM outperform each other in certain areas. In general, GPCP annual estimates exceed the TRMM estimates from 15°N to 15°S. It is reassuring, however, that the seasonal cycle of precipitation using monthly averages is usually consistent between datasets.

On the other hand, the assumption that monthly precipitation fields based solely on gauge data are necessarily more accurate than satellite estimates may be ill founded. Gauge coverage over Africa is sparse (McCollum et al. 2000) and the data that are present may not be accurate. For example, in the eastern Horn (point J of Fig. 6), GPCP averages 622 mm yr^{-1} and agrees well with both TRMM and FEWS NET. Yet, at a nearby station (Mandera, Kenya; 3.9°N, 41.8°E), the annual mean based on the period 1946–72 is only 228 mm yr^{-1} (Griffiths 1972). One recurring problem is that gauge data may be biased low if missing daily values are set to zero when calculating monthly totals, as is, unfortunately, common practice (e.g., Liebmann and Allured 2005). On the positive side, GPCP and TRMM agree well, for the

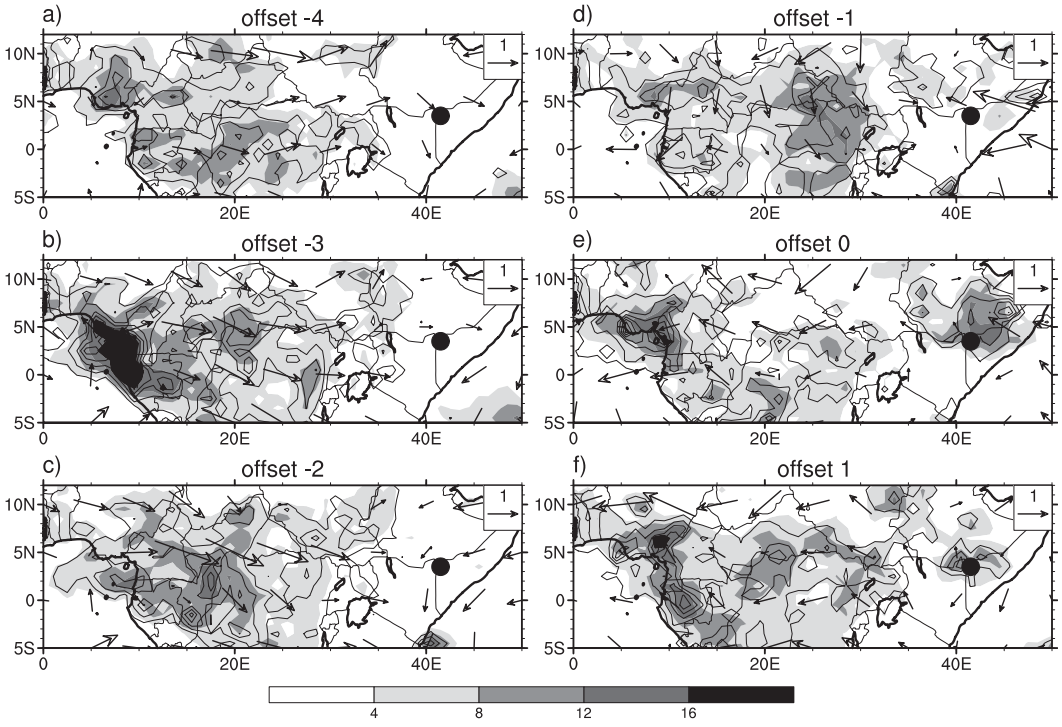

FIG. 18. As in Fig. 17 but for the September–December wet season.

most part, in their estimates of average onset date, consistent with their agreement in the phasing of the annual cycle.

Although the results presented here are based on only 12 years of data and should thus be viewed with some caution, we believe the methodology developed here will be useful to enhance our understanding of the African wet season and its year-to-year variability and thus to improve monsoon prediction.

Acknowledgments. The authors appreciate the excellent suggestions from both anonymous reviewers. We also acknowledge partial support from NOAA CPO MAPP Projects NA100AR4310170 and GC10-685. Author IB was funded by Grant CGL2009-06944 DEVIAJE of the Spanish MICINN.

REFERENCES

Ati, O. F., C. J. Stigter, and E. O. Oladipo, 2002: A comparison of methods to determine the onset of the growing season in northern Nigeria. *Int. J. Climatol.,* **22,** 731–742.

Bowden, J. H., and F. H. M. Semazzi, 2007: Empirical analysis of intraseasonal climate variability over the Greater Horn of Africa. *J. Climate,* **20,** 5715–5731.

Camberlin, P., and N. Philippon, 2002: The east African March–May rainy season: Associated atmospheric dynamics and predictability over the 1968–97 period. *J. Climate,* **15,** 1002–1019.

——, and M. Diop, 2003: Application of daily rainfall principal component analysis to the assessment of the rainy season characteristics in Senegal. *Climate Res.,* **23,** 159–169.

Cheung, W. H., G. B. Senay, and A. Singh, 2008: Trends and spatial distribution of annual and seasonal rainfall in Ethiopia. *Int. J. Climatol.,* **29,** 1723–1734.

Cook, K. H., 2000: The South Indian convergence zone and interannual rainfall variability over southern Africa. *J. Climate,* **13,** 3789–3804.

Dai, A., and K. E. Trenberth, 2002: Estimates of freshwater discharge from continents: Latitudinal and seasonal variations. *J. Hydrometeor.,* **3,** 660–687.

Dinku, T., P. Ceccato, E. Grover-Kopec, M. Lemma, S. J. Connor, and C. F. Ropelewski, 2007: Validation of satellite rainfall products over East Africa's complex topography. *Int. J. Remote Sens.,* **28,** 1503–1526.

El-Fadel, M., Y. El-Sayegh, I. El-Fadel, and D. Khorbotly, 2003: The Nile River Basin: A case study in surface water conflict resolution. *J. Nat. Resour. Life Sci. Educ.,* **32,** 107–117.

Flaounas, E., S. Janicot, S. Bastin, and R. Roca, 2010: The West African monsoon onset in 2006: Sensitivity to surface albedo, orography, SST and synoptic scale dry-air intrusions using WRF. *Climate Dyn.,* **38,** 965–983.

Griffiths, J. F., 1972: The Horn of Africa. *Climates of Africa*, J. F. Griffiths, Ed., Elsevier, 133–165.

Hagos, S. M., and K. H. Cook, 2007: Dynamics of the West African monsoon jump. *J. Climate,* **20,** 5264–5284.

Hoerling, M., J. Hurrell, J. Eischeid, and A. Phillips, 2006: Detection and attribution of twentieth-century northern and southern African rainfall change. *J. Climate,* **19,** 3989–4008.

Huffman, G. J., R. F. Adler, M. M. Morrissey, S. Curtis, R. Joyce, B. McGavock, and J. Susskind, 2001: Global precipitation at

one-degree daily resolution from multi-satellite observations. *J. Hydrometeor.,* **2,** 36–50.

Hutchinson, P., 1992: The Southern Oscillation and prediction of ''Der'' season rainfall in Somalia. *J. Climate,* **5,** 525–531.

International Research Network, 2005: Grain production in Kenya 2005. Export Processing Zones Authority, 16 pp. [Available online at http://www.epzakenya.com/UserFiles/File/GrainReport.pdf.]

Janicot, S., and Coauthors, 2008: Large-scale overview of the summer monsoon over West Africa during the AMMA field experiment in 2006. *Ann. Geophys.,* **26,** 2569–2595.

——, F. Mournier, N. M. J. Hall, S. Leroux, B. Sultan, and G. N. Kiladis, 2009: Dynamics of the West African monsoon. Part IV: Analysis of 25–90-day variability of convection and the role of the Indian monsoon. *J. Climate,* **22,** 1541–1565.

Janowiak, J. E., 1988: An investigation of interannual rainfall variability in Africa. *J. Climate,* **1,** 240–255.

Kiladis, G. N., and H. F. Diaz, 1989: Global climatic anomalies associated with extremes in the Southern Oscillation. *J. Climate,* **2,** 1069–1090.

Kummerow, C., W. Barnes, T. Kozu, J. Shiue, and J. Simpson, 1998: The Tropical Rainfall Measuring Mission (TRMM) sensor package. *J. Atmos. Oceanic Technol.,* **15,** 809–817.

Le Barbé, L., T. Lebel, and D. Tapsoba, 2002: Rainfall variability in West Africa during the years 1950–90. *J. Climate,* **15,** 187–202.

Lebel, T., and Coauthors, 2010: The AMMA field campaigns: Multiscale and multidisciplinary observations in the West African region. *Quart. J. Roy. Meteor. Soc.,* **136,** 8–33.

Liebmann, B., and J. A. Marengo, 2001: Interannual variability of the rainy season and rainfall in the Brazilian Amazon Basin. *J. Climate,* **14,** 4308–4318.

——, and D. Allured, 2005: Daily precipitation grids for South America. *Bull. Amer. Meteor. Soc.,* **86,** 1567–1570.

——, I. Bladé, N. A. Bond, D. Gochis, D. Allured, and G. T. Bates, 2008: Characteristics of North American summertime rainfall with emphasis on the monsoon. *J. Climate,* **21,** 1227–1294.

Marteau, R., V. Moron, and N. Philippon, 2009: Spatial coherence of monsoon onset over western and central Sahel (1950–2000). *J. Climate,* **22,** 1313–1324.

McCollum, J. R., A. Gruber, and M. B. Ba, 2000: Discrepancy between gauges and satellite estimates of rainfall in equatorial Africa. *J. Appl. Meteor.,* **39,** 666–678.

Mekonnen, A., C. D. Thorncroft, A. R. Aiyyer, and G. N. Kiladis, 2008: Convectively coupled Kelvin waves over tropical Africa during the boreal summer: Structure and variability. *J. Climate,* **21,** 6649–6667.

Mounier, F., S. Janicot, and G. N. Kiladis, 2008: The West African monsoon dynamics. Part III: The quasi-biweekly zonal dipole. *J. Climate,* **21,** 1911–1928.

Nicholson, S. E., 1980: The nature of rainfall fluctuations in subtropical West Africa. *Mon. Wea. Rev.,* **108,** 473–487.

——, 1993: An overview of African rainfall fluctuations of the last decade. *J. Climate,* **6,** 1463–1466.

——, M. B. Ba, and J. Y. Kim, 1996: Rainfall in the Sahel during 1994. *J. Climate,* **9,** 1673–1676.

Ogallo, L. J., J. E. Janowiak, and M. S. Halpert, 1988: Teleconnection between seasonal rainfall over East Africa and global sea surface temperature anomalies. *J. Meteor. Soc. Japan,* **66,** 807–822.

Redelsperger, J.-L., C. D. Thorncroft, A. Diedhiou, T. Lebel, D. J. Parker, and J. Polcher, 2006: African Monsoon Multidisciplinary Analysis: An international research project and field campaign. *Bull. Amer. Meteor. Soc.,* **87,** 1739–1746.

Senay, G. B., K. Asante, and G. Artan, 2009: Water balance dynamics in the Nile Basin. *Hydrol. Processes,* **23,** 3675–3681, doi:10.1002.hyp.7364.

Sivakumar, M. V. K., 1988: Predicting rainy season potential from the onset of rains in the Sahelian and Sudanian climatic zones of West Africa. *Agric. For. Meteor.,* **42,** 295–305.

——, 1992: Empirical analysis of dry spells for agricultural applications in West Africa. *J. Climate,* **5,** 532–539.

Sultan, B., and S. Janicot, 2003: The West African monsoon dynamics. Part II: The ''preonset'' and ''onset'' of the summer monsoon. *J. Climate,* **16,** 3407–3427.

Tadross, M. A., B. C. Hewetson, and M. T. Usman, 2005: The interannual variability of the onset of the Maize growing season over South Africa and Zimbabwe. *J. Climate,* **18,** 3356–3372.

Wang, H., and R. Fu, 2007: The influence of Amazon rainfall on the Atlantic ITCZ through convectively coupled Kelvin waves. *J. Climate,* **20,** 1188–1201.

Williams, A. P., and C. Funk, 2011: A westward extension of the warm pool leads to a westward extension of the Walker circulation, drying eastern Africa. *Climate Dyn.,* **37,** 2417–2435.

Zeng, X., and E. Lu, 2004: Globally unified monsoon onset and retreat indexes. *J. Climate,* **17,** 2241–2248.

Zhang, S., and B. Wang, 2008: Global summer monsoon rainy seasons. *Int. J. Climatol.,* **28,** 1563–1578.